Proceedings of the ASME 2014 Conference on Smart Materials, Adaptive Structures and Intelligent Systems
SMASIS2014
September 8-10, 2014, Newport, Rhode Island, USA

SMASIS2014-7536

A SOFT COMBUSTION-DRIVEN PUMP FOR SOFT ROBOTS

Constantinos Stergiopulos[1,2], Daniel Vogt[1,2], Michael T. Tolley[1,2], Michael Wehner[1,2], Jabulani Barber[3], George M. Whitesides[2,3], Robert J. Wood[1,2]

[1]School of Engineering and Applied Science, Harvard University 60 Oxford Street, Cambridge, MA 02138

[2]Wyss Institute for Biologically Inspired Engineering, Harvard University 3 Blackfan Circle, Boston, MA 02115

[3]Department of Chemistry and Chemical Biology, Harvard University 12 Oxford Street, Cambridge, MA 02138

ABSTRACT

This paper describes the design and manufacture of a monolithic high-pressure diaphragm pump made entirely of soft elastomer material and driven by a combustion chamber incorporated within the soft pump structure. The pump can deliver pressures up to 60 kPa and can reach output flows up to 40 ml/min. Methane (CH_4) combustion is used as the actuation source. The pump uses two soft flap-structured check valves for directing the flow. Pumping pressure and frequency dependence were measured and analyzed. Results show that controlled and repeatable combustion of methane is possible without damaging the soft structure. Experimentally, 6-10% methane is identified as the ideal air-fuel ratio for combustion. With continuous delivery of reactants, a 1 Hz pumping frequency was achieved. The volume of the combustion chamber and the material stiffness are identified to be major determinants of the stroke volume.

1. INTRODUCTION

Soft pumps have been developed primarily for microscale applications, because they offer a number of advantages compared to traditional silicon-substrate micropumps, such as low fabrication cost, high compliance and excellent biocompatibility [1]. Soft micropumps are most typically made using poly-dimethylsiloxane (PDMS), taking advantage of established manufacturing techniques developed for microfluidics, e.g. soft lithography over SU-8 photoresist and layer bonding with uncured polymer or oxygen plasma surface treatment [2]. The flow rates and pressures achievable with soft micropumps are, however, limited: flow rates are in the microliter scale and pressures do not exceed 5 kPa [3].

The soft pump presented here aims to reach higher pressures (above 50 kPa) and flows (above 40 ml/min), thus being suitable for larger scale applications, such as driving soft pneumatic actuators (Pneu-Nets) [4]. Pneu-Nets are currently driven by traditional hard shell pumps. Since the pump presented here is entirely soft, it could be embedded directly in a soft robot, resulting in a monolithic design with reduced interfaces and rigid components [5,6].

2. PUMPING PRINCIPLE

The soft combustion-driven pump operates by causing a membrane to deflect into and out of a pumping chamber, effectively changing the volume of the chamber (Fig. 1a). Check valves at the inlet and outlet of this chamber enforce unidirectional flow. Most of diaphragm micropumps use electrostatic, magnetic force or piezo-electric materials to deflect the membrane [3]. In this paper and in view of delivering high pressures and flows, we use the combustion of methane (CH_4) as actuation source. Due to its high energy density, combustion has been previously used for directly actuating soft robots, such as robot jumpers [7,8], but never for driving a soft pump. Combustion is an exothermic reaction between a hydrocarbon and oxygen that creates carbon dioxide, water (vapor) and heat. For methane, the combustion with air gives the following stoichiometric reaction (1):

$$CH_4 + 2O_2 + 3.76N_2 \rightarrow CO_2 + 2H_2O + 3.76N_2 - 891\text{kJ/mol} \quad (1)$$

where the energy is released as heat. Air was used instead of pure oxygen, as the higher reactivity of the latter makes it challenging to stock safely. Using air leads to a reduced exothermal reaction, as all the Nitrogen (N_2) in the air is not taking part in the combustion. Methane was preferred over the other hydrocarbons such as butane or propane because the combustible range of the air-fuel mixture ratio for methane is larger (i.e. between 5 and 15% of methane in mixture) [9]. The explosive mixture is brought in the combustion chamber and is

ignited using a spark from a high voltage source (~1000V). The carbon dioxide (CO_2) and vapor (H_2O) are evacuated through the exhaust (Fig. 1b), and replaced by the reactants (methane and air) for the next explosion.

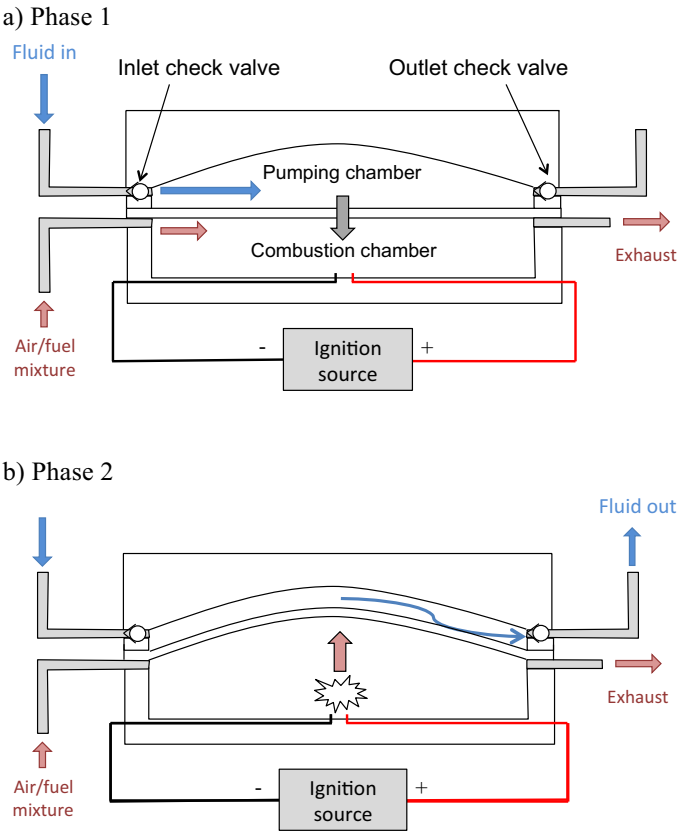

Figure 1. Schematic diagram of the combustion-driven soft pump. a) Phase 1: Fluid enters pumping chamber as membrane returns to horizontal position. b) Phase 2: Membrane deflects due to the combustion reaction, pushing the fluid out.

3. FABRICATION

The pump is made out of six silicone rubber parts (Fig. 2a). To manufacture these parts, molds were 3D printed using an Objet Connex 500. Silicone rubber was poured in the different molds, degassed and cured at 60°C for 15 minutes. Two different silicone rubbers were tested experimentally: Dragon Skin 20 (Shore hardness 20 A; Smooth-On Inc.) and Sorta Clear 40 (Shore hardness 40 A; Smooth-On Inc). Parts were glued together using SilPoxy glue (Smooth-On Inc.). Polyurethane (PU) tubing was used for the different inlets/outlets and was similarly glued to the structure. SilPoxy glue is a simple bonding method, but it was noticed during the experiments that it did not guarantee impermeability at high pressures. Thus, for improved sealing, an encapsulation layer of e rubber was added all around the structure. Fig. 2a and Fig. 2b depict an exploded view of the pump (without the encapsulation), and a picture of the finished product, respectively. The pump's central circular structure has a 50 mm diameter and a total height of 25 mm. The combustion chamber and pumping chamber have volumes of 7 ml and 6 ml respectively. The latter also represents the pump's maximal theoretical stroke volume.

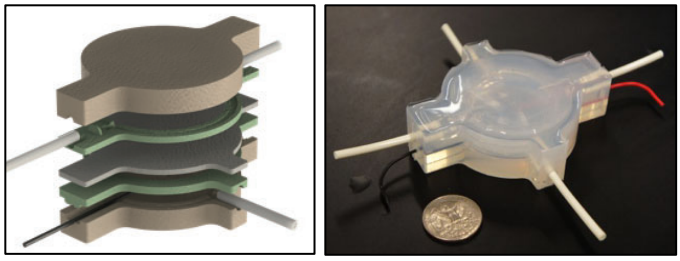

Figure 2. Left: exploded view of the different pump layers. Right: picture of the final product including the encapsulation layer and soft check valves.

Soft check valves were manufactured and tested independently. A flap and stopper structure was chosen for the mechanism, as it was successfully used in previous designs for microvalves [10]. Figure 3 illustrates the two parts that form the one-way valve. One part contains the flap and the other the stopper. The valves have dimensions of 40 mm x 10 mm x 8 mm. Both parts and tubing are connected again using silicone glue.

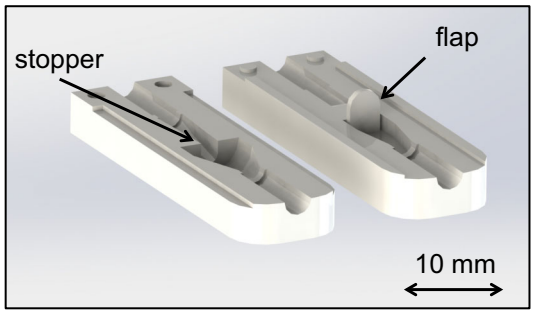

Figure 3. SolidWorks view of the two silicone rubber parts forming the check valve.

4. EXPERIMENTAL SETUPS

4.1 Influence of material stiffness on chamber compliances

A first experiment was conducted to characterize the pump's softness (volume compliance). Two pumps were manufactured with the two silicone rubber materials stated previously. In both cases, the membrane was made out of Dragon Skin 20. The combustion chamber and pumping chamber were filled with water and the inlet and outlets were blocked. A syringe was used to add progressively water in the combustion chamber and two digital pressure gauges (DPG1000-B, Omega Engineering Inc.) were used to measure

the pressure increase in both chambers. Measurements were taken for every milliliter injected, from 0 to 20 milliliters.

The check valves were first characterized separately. They were made using Sorta Clear 40. Molds were designed in a way that there is no gap between the flap and the stopper when there is no flow. Two flap thicknesses were tested: 800 µm and 1 mm. Tests were carried out with water as working fluid to facilitate volume/flow rate measurements. Water was injected at different flow rates and pressure at the input was measured using a pressure gauge. The output flow rate was measured by timed collection of the water in a graded recipient. Measurements were also done for backflow by connecting the water source to the output and measuring flow at the input.

4.2 Influence of combustion chamber pressure and frequency on flow rate

In order to find optimal working frequencies and pressures for the pump, these parameters were varied and the output flow was measured for each case. For these tests, the pump used had a Sorta Clear 40 body and a Dragon Skin 20 membrane. The working fluid, in this case pressurized air, whose pressure was controlled using a pressure regulator to be in the range of 0 to 68 kPa (10 psi) with an accuracy up to 0.5 kPa (0.08 psi). The pumping frequency was controlled by two solenoid valves (VSO Low Flow, Parker Hannifin Corp.). To assure filling and emptying at two distinct phases, the valves were working always in opposite states (when one is open the other is closed and vice versa, Fig. 4). The valves were controlled using an Arduino Uno board (Arduino, Smart Projects). Water was used again as working fluid and output flow was measured similarly as in the previous experiments. Figure 4 shows a schematic of the experimental setup.

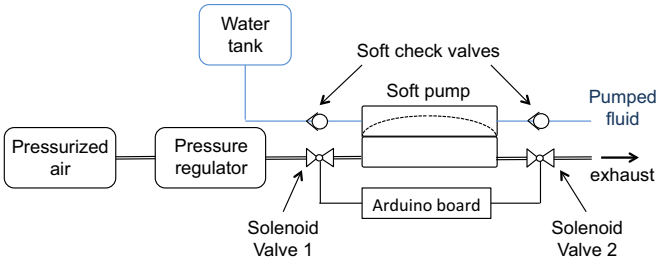

Figure 4. Experimental setup for pump characterization. A pressure regulator and two solenoid valves are used to control pumping pressure and frequency respectively.

For the pumping pressure dependency tests, the pressure was varied from 0 to 40 kPa and the measurements were done for pumping frequencies of 0.25 Hz, 0.5 Hz and 1 Hz. For the frequency dependency, the frequencies tested varied from 0.1 Hz to 5 Hz and the tests were done for 14 kPa, 24 kPa and 35 kPa. Every experiment was performed four times, to compute mean values and standard deviations for each test.

4.3 Characterization of air-fuel mixture and membrane deflection

For tests with combustion, the air-fuel ratio was controlled precisely in order to yield an explosive mixture. To accurately inject the appropriate mixture of methane and air into the combustion chamber, two mass flow controllers (MFCs) were used (1179A Mass-Flo, MKS Instruments Inc.), one for methane and one for air (Fig. 5). The MFCs were controlled using a MKS 247D four-channel readout (MKS Instruments Inc.), which allowed output flow rates from 0 to 840 standard cubic centimeters per minute (sccm). Both outputs were connected with a Y connector and the mixture of air and fuel mixture was continuously injected into the combustion chamber. The exhaust on the other side of the chamber was left open, so that the products of the chemical reaction could exit the chamber and be replaced by the reactants for the next explosion. A manual spark (Olympian GM-3X, Camco Manufacturing Inc.) was periodically sparking at the chosen frequency to trigger the explosions. For the spark, two electric cables were inserted into the middle of the combustion chamber (through the rubber structure) with their tips separate by a 4 mm gap.

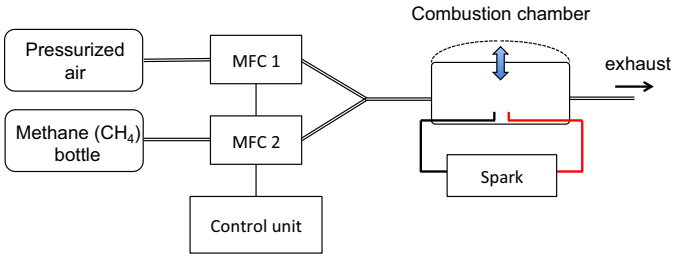

Figure 5. Experimental setup for the combustion tests. Mass flow controllers were used to control air and methane flows and provide a stoichiometrically appropriate mixture for combustion.

First, different air-fuel ratios were tested in order to establish the range of mixture ratios yielding explosions. Mixture ratios from 5%-15% methane were tested with the airflow remaining constant at 200 sccm. In a second test, the mixing ratio is fixed at 7.8% CH_4 and total flow is varied from 200 sccm to 800 sccm. Finally, some tests were conducted to study the effects of other parameters, such as the membrane material and the volume of the combustion chamber. For the materials, Ecoflex 00-30 and Dragon Skin 20 were tested, and for the combustion chamber's volume, two volumes were tested: 5 and 6 ml. The explosion was characterized by the max vertical deformation of the chamber's membrane: explosions were filmed with a high-speed camera (Phantom v7.3, Vision Research Inc.), which was set at 3000 frames/sec. A ruler was placed on the side in order to directly measure the deformation on the image obtained from the high-speed camera.

5. RESULTS AND DISCUSSION

Figure 6 shows the pressure-volume diagrams of the pressure (combustion) and pumping chamber, for the Dragon Skin 20 pump (left) and Sorta Clear 40 pump (right). Results show that for 20 ml injected, the pumping chamber can reach 15 kPa and 42 kPa, respectively, and that the pressure-volume relationship is linear, suggesting a relatively constant compliance over the entire pressure range.

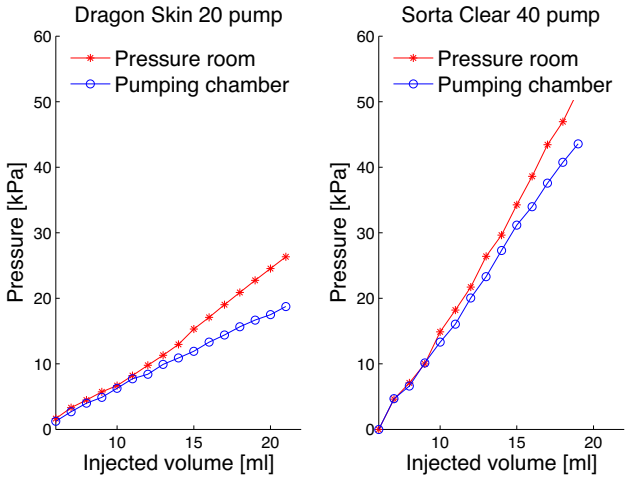

Figure 6. Pressure (kPa) versus injected volume of water (ml) for both pressure (combustion) chamber and pumping chamber.

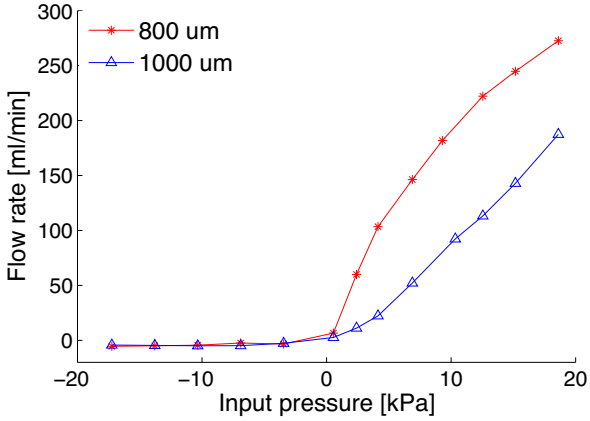

Figure 7. Typical diagram for flow rate versus input pressure for check valves with flap thicknesses of 800 µm and 1 mm.

Pressures reached with the Sorta Clear 40 pump are almost twice as large as those with the Dragon skin for the same injected volume. This is expected, because Sorta Clear is stiffer, which leads to less structure deformation and therefore steeper pressure increase. Figure 7 shows the results obtained for the designed (one-way) check valves. From the graphs, the valves fluidic resistance $R_{v,+} = \Delta P/\Delta Q$ was estimated (i.e. for the 800 µm flap model $R_{v,+} = 0.093$ kPa min/ml). Although, the backflow resistance should be infinite in theory, during the experiments there was some backflow leakage. For the 800 µm flap, the backflow resistance was estimated at $R_{v,-} = 3.16$ kPa min/ml.

Fig. 8 shows the dependence of output flow rate on pumping pressure (maximum pressure in the pumping chamber). The continuous line gives the mean value of the repeated measurements and shaded zone represents the standard deviation.

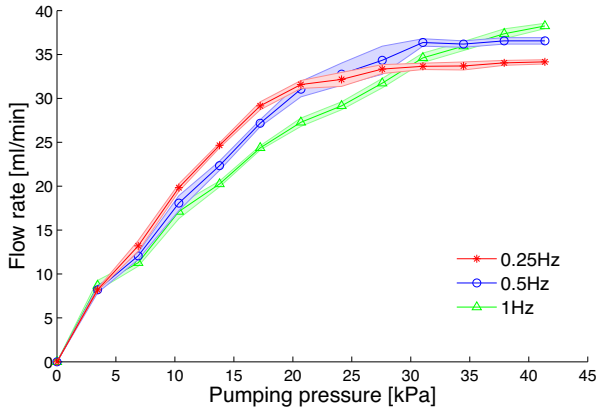

Figure 8. Flow rate as a function of pressure for pumping frequencies of 0.25 Hz, 0.5 Hz and 1 Hz.

At low pressures (between 0 and 20 kPa), for all curves, the flow rate increases linearly with maximum pressure in the pressure chamber. At higher pressures, the flow rate saturates because, at some point, the membrane is entirely in contact with the upper wall, meaning that the pump reaches the maximum possible stroke volume at each cycle. It is noticeable that this saturation occurs at higher pressures for higher pumping frequencies. Maximum flow rate is also higher in higher frequencies. For instance, max flow rate for 0.25 Hz pumping is 34.2 ml/min whereas for 0.5 Hz pumping the maximal flow rate obtained is 36.6 ml/min, however, the proportionality implied by the simple rule: flow rate equals stroke volume times frequency is not respected, most likely due to limitation in achieving maximum stroke volume at high frequencies.

Figure 9 shows the results obtained for the frequency dependency tests. For a pumping pressure of 13.8 kPa, the maximal flow rate was obtained at 0.25 Hz and was equal to 24.5 ml/min. As the pressure increases, the membrane is deflected more rapidly, meaning that the maximal flow can be reached at higher frequencies. For instance, at a pumping pressure of 34.5 kPa, maximal flow rate was obtained at 0.67 Hz and the resulting flow rate reached 38.5 ml/min. When over-increasing the pumping frequency, the membrane does not have enough time to push all the liquid out of the pumping chamber, leading to a less efficient working mode.

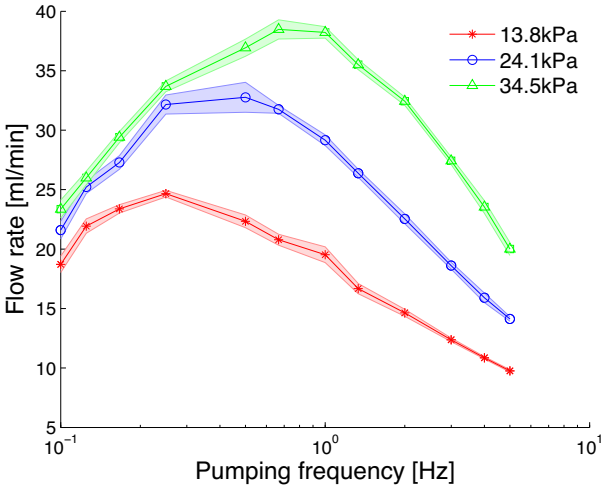

Figure 9. Flow rate according to pumping frequency for pumping pressures of 13.8 kPa, 24.1 kPa and 34.5 kPa.

Combustion experiments showed that there is combustion only if the ratio of CH_4 in the air-methane mixture is between 6.5% and 10%, which is a smaller range than in theory (5% to 15%) and if the methane ratio is too lean or too rich, there is no reaction at all. Figure 10 shows the number of explosions per minute achieved upon continuous sparking for the different air-fuel ratios (with input flow of 200 sccm). Within the combustible range, there were about 3 explosions per minute. The highest combustion frequency was obtained for a ratio of 7.8% methane.

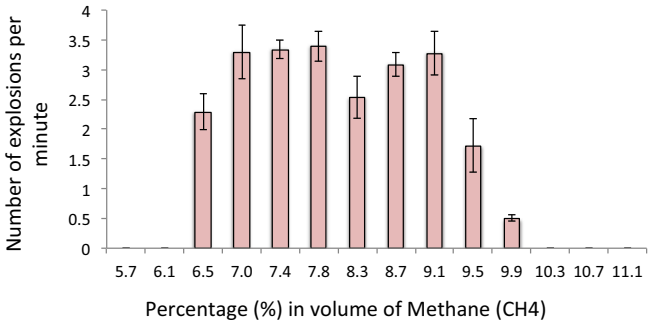

Figure 10. Explosions per minute for different air-fuel mixtures while sparking continuously. Error bars represent measurements' standard deviation.

Figure 11 below shows the number of combustions per minute for different input flows, all being 7.8% methane air-fuel mixtures. With airflow of 800 sccm, the combustion frequency reaches 15.8 explosions per minute (0.26 Hz). These measurements were done while continuously sparking with the manual spark. When sparking continuously, some small explosions happen locally in the combustion chamber before the chamber is filled entirely with the combustible mixture. This causes a delay between main explosions leading to smaller combustion frequencies. In fact, when triggering the spark with intervals, it is possible to increase substantially the combustion frequency and we were able to reach a frequency of 1 Hz with a 800 sccm input flow.

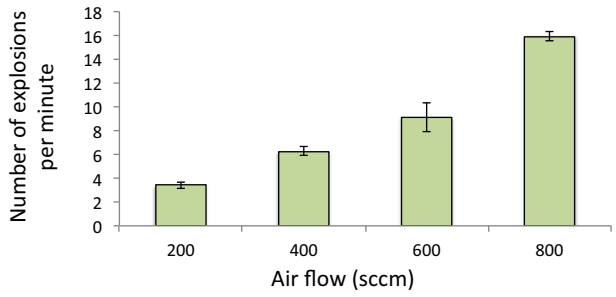

Figure 11. Explosions per minute for input flows varying from 200 sccm to 800 sccm with continuous sparks.

A high-speed camera was used to film and visualize the deflection of the membrane during the explosion. Tests were performed on two combustion chambers, one with a Dragon Skin 20 and one with Ecoflex 00-30 membrane, both chambers having an identical volume chamber of 5 milliliters. The Dragon Skin 20 membrane had a mean maximal deflection of 9.4 mm, while the Ecoflex reached a deflection of 17.6 mm. Figure 12 shows screenshots of the explosions from the high-speed video at 10 millisecond intervals.

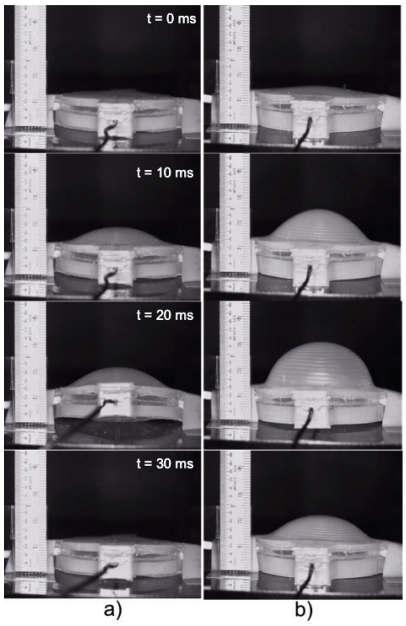

Figure 12. Membrane deflection due to combustion after 10, 20 and 30 milliseconds for Dragon Skin 20 (a) and Ecoflex 00 30 (b) membranes.

Using these videos it is possible to measure that the whole reaction and membrane deflection lasts for about 50

milliseconds. For the 6 ml chamber that also uses an Ecoflex 00-30 membrane, the maximal vertical deflection reached a higher level (22.2 mm) as compared to the 5 ml chamber. The increase in maximal deflection is proportional to the increase in chamber volume (22.2 mm ≈ 17.6 mm x 6 ml/5 ml) and this is expected because the elastic structure is quasi-linear and the energy released from the exothermic reaction is linearly depending on the number of moles in the reaction, thereby linearly dependent on chamber volume.

6. CONCLUSIONS

The soft pump presented in this paper operates at higher pressures and flows than previously demonstrated soft micropumps, making it ideal for driving Pneu-Nets actuators and other applications requiring similar characteristics. Moreover, the pump is scalable, the limiting factor being the resolution of the 3D-printed molds when going to smaller scales. A solution in this case would be to make the molds in another material using other machining or photolithography techniques. The manufacturing method is simple, straightforward and easily reproducible. Although testing was performed with water, this pump also works with gases. The pump can be made with different silicone rubbers. As seen in the results, using softer materials makes the overall structure more flexible and stretchable but less efficient, as a lot of the pumping pressure is used for deforming the bulk structure rather than solely the membrane.

The most innovative part of this research is the use of methane combustion to drive the pump. It is possible to get repetitive explosions with relatively high frequency. It is also possible to control membrane deflection and thus implicitly stroke volume by varying system parameters, such as chamber geometry and material properties. This research can be used as a starting point for designing an entirely soft combustion pump.

REFERENCES

[1] Ni J., Huang F., Wang B., Li B., and Lin Q, 2010. “A planar PDMS micropump using in-contact minimized-leakage check valves”, *Journal of Micromechanics and Microengineering*, vol. 20.

[2] Jeon N.L., Chiu D. T., Wargo C. J., Wu H., I. Choi S., Anderson J. R., and Whitesides G. M., 2002. “Design and fabrication of integrated passive valves and pumps for flexible polymer 3-dimensional microfluidic systems,” *Biomedical microdevices*, vol. 4:2, pp. 117–121.

[3] Nisar A., Afzulpurkar N., Mahaisavariya B., and Tuantranont A., 2007. “MEMS-based micropumps in drug delivery and biomedical applications”, *Sensors and Actuators B 130*, pp. 917–942.

[4] Shepherd R. F., Ilievski F., Choi W., Morin S. A., Stokes A. A., Mazzeo A. D., Chen X., Wang M., and Whitesides G. M., 2011. “Multigait soft robot,” *Proc. Nat. Acad. Sci.*, vol. 108, no. 51, pp. 20400–20403.

[5] Tolley M. T., Shepherd R. F., Mosadegh B., Galloway K. C., Wehner M., Karpelson M., Wood R. J., Whitesides G. M., under review. “A Resilient, Untethered Soft Robot”, *Soft Robotics*.

[6] Shepherd R. F., Stokes A. A., Freake J., Barber J., Snyder P. W., Mazzeo A. D., Cademartiri L., Morin S. A., and Whitesides G. M., 2013. “Using explosions to power a soft robot,” *Angewandte Chemie*, vol. 125, pp. 2964–2968.

[7] Laser D. J., Santiago J. G., 2004. “A review of micropumps”, *Journal of Micromechanics and Microengineering*, pp. R35-R64.

[8] Tolley M. T., Shepherd R. F., Karpelson M., Bartlett N. W., Galloway K. C., Wehner M., Nunes R., Whitesides G. M., Wood R. J., 2014. “An untethered jumping soft robot”, *International Conference on Intelligent Robots and Systems (IROS)*.

[9] Cashdollar K. L., Zloshower I. A., Green G. M., Thomas R. A., and Hertzberg M., 2000. “Flammability of methane, propane, and hydrogen gases”, *Journal of Loss Prevention in the Process Industries 13*, pp. 327–340.

[10] Yang B., and Lin Q., 2016. “Planar micro-check valves explointing large polymer compliance”, *Journal of Sensors and Actuators A 134*, pp. 186–193.